



## In-situ biogas upgrading in thermophilic granular UASB reactor: key factors affecting the hydrogen mass transfer rate

**Bassani, Ilaria; Kougias, Panagiotis; Angelidaki, Irini**

*Published in:*  
Bioresource Technology

*Link to article, DOI:*  
[10.1016/j.biortech.2016.09.083](https://doi.org/10.1016/j.biortech.2016.09.083)

*Publication date:*  
2016

*Document Version*  
Peer reviewed version

[Link back to DTU Orbit](#)

*Citation (APA):*  
Bassani, I., Kougias, P., & Angelidaki, I. (2016). In-situ biogas upgrading in thermophilic granular UASB reactor: key factors affecting the hydrogen mass transfer rate. *Bioresource Technology*, 221, 485-491.  
<https://doi.org/10.1016/j.biortech.2016.09.083>

---

### General rights

Copyright and moral rights for the publications made accessible in the public portal are retained by the authors and/or other copyright owners and it is a condition of accessing publications that users recognise and abide by the legal requirements associated with these rights.

- Users may download and print one copy of any publication from the public portal for the purpose of private study or research.
- You may not further distribute the material or use it for any profit-making activity or commercial gain
- You may freely distribute the URL identifying the publication in the public portal

If you believe that this document breaches copyright please contact us providing details, and we will remove access to the work immediately and investigate your claim.

1 **In-situ biogas upgrading in thermophilic granular UASB**  
2 **reactor: key factors affecting the hydrogen mass transfer rate**

3 Ilaria Bassani, Panagiotis G. Kougias<sup>\*</sup>, Irimi Angelidaki

4 Department of Environmental Engineering, Technical University of Denmark, Kgs.

5 Lyngby, Denmark

6

7 <sup>\*</sup>Corresponding author: Panagiotis G. Kougias, Department of Environmental

8 Engineering, Technical University of Denmark, Bld 113, 2800 Lyngby, Denmark.

9 E-mail address: panak@env.dtu.dk, Tel.: +45 45251454

10 **Highlights**

- 11 • Biogas upgrading to 82% CH<sub>4</sub> is feasible in a thermophilic granular UASB reactor.
- 12 • H<sub>2</sub> is introduced in a separate chamber having a volume of 25% the reactor.
- 13 • H<sub>2</sub> low gas-liquid mass transfer rate limits the availability of H<sub>2</sub> for methanogens.
- 14 • H<sub>2</sub> distribution can be improved using porous inert devices, like ceramic sponge.
- 15 • Gas recirculation and chamber configuration help to maximize CO<sub>2</sub> conversion to
- 16 CH<sub>4</sub>.

17

18 **Abstract**

19 Biological biogas upgrading coupling CO<sub>2</sub> with external H<sub>2</sub> to form biomethane opens  
20 new avenues for sustainable biofuel production. For developing this technology  
21 efficient H<sub>2</sub> to liquid transfer is fundamental. This study proposes an innovative setup  
22 for in-situ biogas upgrading converting the CO<sub>2</sub> in the biogas into CH<sub>4</sub>, via  
23 hydrogenotrophic methanogenesis. The setup consisted of a granular reactor connected  
24 to a separate chamber, where H<sub>2</sub> was injected. Different packing materials (rashig rings  
25 and alumina ceramic sponge) were tested to increase gas-liquid mass transfer. This  
26 aspect was optimized by liquid and gas recirculation and chamber configuration. It was  
27 shown that by distributing H<sub>2</sub> through a metallic diffuser followed by ceramic sponge in  
28 a separate chamber, having a volume of 25% of the reactor, and by applying a mild gas  
29 recirculation, CO<sub>2</sub> content in the biogas dropped from 42 to 10% and the final biogas  
30 was upgraded from 58 to 82% CH<sub>4</sub> content.

31

32 **Keywords**

33 In-situ biogas upgrading; Hydrogen; Gas-liquid mass transfer rate; UASB; Granules;  
34 Anaerobic digestion

35

## 36 **1. Introduction**

37 Anaerobic Digestion (AD) of organic waste is a promising technology for sustainable  
38 energy production (Weiland, 2010). The potato-starch processing industry produces, as  
39 byproduct, up to 1 m<sup>3</sup> of potato juice per ton of potatoes (Abeling and Seyfried, 1993).  
40 Potato-starch wastewater contains high concentration of biodegradable compounds,  
41 such as starch and proteins, suitable for biogas production via AD (Barampouti et al.,  
42 2005). Biogas typically contains ~50-70% CH<sub>4</sub> and 30-50% CO<sub>2</sub>. Biogas upgrading to  
43 CH<sub>4</sub> content higher than 90% increases its heating value and its potential applications as  
44 alternative to natural gas (Deng and Hägg, 2010).

45 Methods currently available for biogas upgrading are mainly based on  
46 physicochemical CO<sub>2</sub> removal. Nevertheless, these technologies require use of  
47 additional materials and chemicals considerably increasing the cost of the process and  
48 energy input. Alternatively, biogas can be upgraded by biologically coupling H<sub>2</sub>,  
49 derived from water electrolysis, with CO<sub>2</sub> present in the biogas to convert them to CH<sub>4</sub>.  
50 H<sub>2</sub> can be produced using the electricity generated by the surplus of energy from wind  
51 mills or photovoltaic facilities, which may result from variable weather conditions. This  
52 reaction is carried out by a group of microorganisms known as hydrogenotrophic  
53 methanogenic archaea that utilize CO<sub>2</sub>, as carbon source, and H<sub>2</sub>, as electron donor, to  
54 produce CH<sub>4</sub> via hydrogenotrophic methanogenesis (Muñoz et al., 2015). Previous  
55 studies demonstrated that the addition of H<sub>2</sub> to a conventional biogas reactor can lead to

56 20 to 40% increase in CH<sub>4</sub> production rate, as result of the conversion of the CO<sub>2</sub>  
57 present in the biogas to additional CH<sub>4</sub> (Luo and Angelidaki, 2013; Luo et al., 2012).

58 Although biological biogas upgrading offers economical and technical advantages  
59 compared to traditional methods (Nordberg et al., 2012), H<sub>2</sub> mediated biogas upgrading  
60 is still challenging. One of the main limitations is the low H<sub>2</sub> gas-liquid mass transfer  
61 rate (Bassani et al., 2015; Luo and Angelidaki, 2012; Luo et al., 2012).

62 H<sub>2</sub> gas-liquid mass transfer rate can be described by the following equation (1):

$$r_t = 22.4k_L a(H_{2gTh} - H_{2l})$$

63 where  $r_t$  (L/(L-day)) is the H<sub>2</sub> gas-liquid mass transfer rate, 22.4 (L/mol) is the gas  
64 volume to mole ratio (1 mol gas corresponds to 22.4 L at STP),  $k_L a$  (day<sup>-1</sup>) is the gas  
65 transfer coefficient,  $H_{2gTh}$  (mol/L) represent the H<sub>2</sub> concentration in the gas phase while  
66  $H_{2l}$  (mol/L) the H<sub>2</sub> dissolved in the liquid phase. One way to increase H<sub>2</sub> gas-liquid  
67 mass transfer rate is by increasing  $k_L a$ . This coefficient is specific for given reactor  
68 configuration and operating conditions (Pauss et al., 1990). Therefore,  $k_L a$  can be  
69 modulated by changing parameters such as mixing speed (Bhattacharyya and Singh,  
70 2010; Luo and Angelidaki, 2012), gas recirculation (Guiot et al., 2011) and H<sub>2</sub> diffusion  
71 device (Luo and Angelidaki, 2013; Díaz et al., 2015).

72 Besides, high-rate anaerobic treatment using up-flow anaerobic sludge blanket  
73 (UASB) reactors is commonly applied in industrial wastewater treatment plants  
74 (Gomec, 2010; Sevilla-Espinosa et al., 2010). Moreover, typically a UASB process is  
75 expected to provide higher methane content in the biogas than a CSTR process (Nizami  
76 et al., 2012).

77 UASB reactors' technology is based on the presence of granular sludge comprised of  
78 microorganisms responsible for catalyzing the biological conversion of organic matter

79 to biogas. High recirculation flow rates and consequent high up-flow velocities have an  
80 in important role for the hydraulic mixing improving the wastewater to granules contact  
81 (Powar et al., 2013; Zheng et al., 2012). It has been previously reported that  
82 carbohydrate degraders and hydrogenotrophic methanogens are predominant in starch-  
83 grown granules, likely due to their role in the interspecies H<sub>2</sub> transfer with syntrophic  
84 bacteria (Lu et al., 2015). Moreover, previous studies on H<sub>2</sub> mediated biogas upgrading  
85 demonstrated that H<sub>2</sub> affected the microbial community composition enhancing the  
86 hydrogenotrophic methanogenic pathway and the syntrophic relationship between  
87 bacteria and hydrogenotrophic methanogens (Bassani et al., 2015).

88 In this study an innovative setup consisting of a UASB granular reactor connected to  
89 a separate chamber, where the H<sub>2</sub> was injected, was designed to mediate efficient H<sub>2</sub>  
90 transfer to liquid phase for biological conversion of H<sub>2</sub> and CO<sub>2</sub> to CH<sub>4</sub>. Key factors  
91 affecting the H<sub>2</sub> gas-liquid mass transfer rate were evaluated. More specifically, the  
92 effect of different operating conditions aiming in increasing  $k_L a$  of H<sub>2</sub> to gas, and  
93 thereby increase the gas to liquid transfer, were studied to elucidate their role in  
94 improving CO<sub>2</sub> and H<sub>2</sub> conversion to CH<sub>4</sub>. Parameters examined were liquid and gas  
95 recirculation and configuration of diffusion devices. Moreover, the addition of packing  
96 materials as a mean to minimize the gas bubble size and thus increase the gas  
97 dissolution in the liquid was tested. Finally, the effect of gas retention time was  
98 evaluated using single or serial chamber configurations with different working volumes.

99

## 100 **2. Materials And Methods**

### 101 **2.1 Substrate characteristics and feedstock preparation**

102 Potato-starch wastewater substrate was obtained from Karup Kartoffelmelfabrik  
103 potato-starch processing factory, Denmark. Because potato-starch processing involves  
104 an up-concentration step, the provided substrate was diluted 10 times with water and  
105 Basal Anaerobic (BA) medium, to adjust the volatile solids (VS) content to the required  
106 operation conditions. Successively, the substrate was stored at -20°C, in 5 L bottles and  
107 thawed at 4°C for 2-3 days, before usage. BA medium was prepared as described in  
108 Supplementary Information (SI). The diluted substrate had a pH of 6.05, chemical  
109 oxygen demand (COD) of 21.76±0.15 g/L, total solids (TS) and VS content of  
110 26.14±0.17 and 18.73±0.12 g/L, respectively. The concentration of total volatile fatty  
111 acids (VFA) was 49.29±4.94 mg/L. Total Kjeldahl Nitrogen (TKN) and ammonium  
112 nitrogen NH<sup>4+</sup> (NH<sub>4</sub>-N) were 1.24 ± 0.01 and 0.30 ± 0.01 g-N/L, respectively.

113

## 114 **2.2 Setup and operation of the reactors**

115 Each setup was composed of a UASB reactor with a working volume of 1.4 L,  
116 connected to a separate H<sub>2</sub>-injection chamber with a working volume of 0.2 L. The  
117 feeding was introduced from the bottom of the UASB. The reactors were inoculated  
118 with 550 g of mesophilic granules, obtained from Colsen wastewater treatment plant  
119 treating potato starch wastewater (The Netherlands) and BA medium. The granules  
120 were adapted to thermophilic conditions for 25 days by feeding the reactors with diluted  
121 potato starch wastewater at hydraulic retention time (HRT) of 7 days and organic  
122 loading rate (OLR) of 2.79 gVS/L.day. A double net-separator was located in the upper  
123 part of each UASB to prevent the wash out of granules. One setup (R1) was used as  
124 upgrading reactor, while the other (R2) was utilized as control reactor operated  
125 throughout the experiment without H<sub>2</sub> injection. Both reactors were maintained at

126 thermophilic conditions ( $55 \pm 1$  °C) by circulating hot water through a water jacket  
 127 around the UASB reactors glass walls.

128 After the startup phase, the whole experiment was divided in 8 periods. During period I  
 129 the OLR was increased to 3.73 gVS/L day shortening the HRT to 5 days (Pre H<sub>2</sub> phase).  
 130 The recirculation flow rate was set to 4 L/h. From period II, H<sub>2</sub> was continuously  
 131 injected to R1 through a diffuser placed at the bottom of the H<sub>2</sub>-injection chamber (In-  
 132 situ phase). Rashig rings (5 mm internal diameter) were inserted into the separate  
 133 chamber of both reactors to maximize the H<sub>2</sub> gas-liquid mass transfer rate in case of R1.  
 134 The volumetric H<sub>2</sub> flow rate was set to 4 times the CO<sub>2</sub> production rate (in the gas  
 135 phase) recorded before the H<sub>2</sub> addition, according to Luo and Angelidaki (2013b), i.e.  
 136 3.5 L/L.day, and then reduced to improve the H<sub>2</sub> consumption. In period III, the  
 137 recirculation flow rate of both reactors was increased to 7 L/h. Successively, in period  
 138 IV, rashig rings were replaced by an inert alumina ceramic sponge, while in periods V  
 139 and VI different gas recirculation flow were applied. In order to evaluate the effect of  
 140 the gas retention time, the H<sub>2</sub>-injection chamber volume was doubled to 400 mL by  
 141 connecting two chambers in series (Period VII) or by assembling them as a single  
 142 chamber with extended length (Period VIII).

143 The percentage of H<sub>2</sub> utilized was calculated according to the following equation (2):

$$\text{H}_2 \text{ utilization efficiency} = \frac{\text{H}_2 \text{ injected} \left( \frac{\text{L}}{\text{L} - \text{day}} \right) - \text{H}_2 \text{ in biogas} \left( \frac{\text{L}}{\text{L} - \text{day}} \right)}{\text{H}_2 \text{ injected} \left( \frac{\text{L}}{\text{L} - \text{day}} \right)} * 100$$

144 The percentage of CH<sub>4</sub> derived from the conversion of CO<sub>2</sub> and H<sub>2</sub> was calculated  
 145 according to the equation 3:

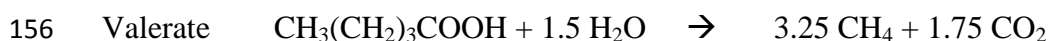
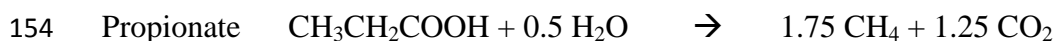


146 CH<sub>4</sub> from CO<sub>2</sub> and H<sub>2</sub> conversion (%) =

147 
$$\left( \frac{(\text{CH}_4 \text{ production rate in R1 } (\frac{\text{L}}{\text{L.day}}) - \text{CH}_4 \text{ production rate in R2 } (\frac{\text{L}}{\text{L.day}}))}{\text{CH}_4 \text{ production rate in R2 } (\frac{\text{L}}{\text{L.day}}) + \text{CH}_4 \text{ production rate equivalent to VFA in R2 } (\frac{\text{L}}{\text{L.day}})} \right) +$$

148 
$$\frac{(\text{CH}_4 \text{ production rate equivalent to VFA in R1 } (\frac{\text{L}}{\text{L.day}}) - \text{CH}_4 \text{ production rate equivalent to VFA in R2 } (\frac{\text{L}}{\text{L.day}}))}{\text{CH}_4 \text{ production rate in R2 } (\frac{\text{L}}{\text{L.day}}) + \text{CH}_4 \text{ production rate equivalent to VFA in R2 } (\frac{\text{L}}{\text{L.day}})} * 100$$

149 Where CH<sub>4</sub> production rate represents the volume of CH<sub>4</sub> produced per liter of  
150 reactor, per day, measured at the outflow of the reactor. While CH<sub>4</sub> production rate  
151 equivalent to VFA was calculated converting VFA concentrations, in the reactors, to  
152 CH<sub>4</sub> production equivalent according the following conversion reactions:



157 This was done to take into account the biomethanation inhibition caused by the injection  
158 of H<sub>2</sub> in the upgrading reactor and provide a more accurate estimation of the CH<sub>4</sub>  
159 produced from the conversion of CO<sub>2</sub> and H<sub>2</sub>.

160

### 161 **2.3 Analytical methods**

162 The biogas production was recorded in daily basis. TS, VS, NH<sub>4</sub>-N and TKN were  
163 measured according to the Standard Methods for Examination of Water and Wastewater  
164 (APHA, 2005). Liquid samples from the reactors were collected for pH and VFA  
165 analysis every second day. VFA and pH were measured according to Kougiyas et al.,  
166 (2015) as described in SI. Detailed description of chromatographs utilized to measure  
167 biogas composition and CH<sub>4</sub> production (for batch assays) are given in SI. Detection  
168 limits for the measurement of CH<sub>4</sub>, CO<sub>2</sub> and H<sub>2</sub> by GC were defined by the calibration  
169 curve (5–100%), while the detection limits for VFA were 5–1500 mg/L.

170

## 171 **2.4 Specific methanogenic activity test**

172 Specific methanogenic activity (SMA) assays were conducted during reactors' steady  
173 state operation. 1 g of granules and 9 mL of liquid sample obtained from the reactors  
174 were immediately transferred to 36 ml serum bottles under anaerobic conditions. The  
175 bottles were supplemented with acetate (20 mM) or H<sub>2</sub>/CO<sub>2</sub> (80:20, 1 atm). Bottles with  
176 glucose (10 mM) or water as substrate were prepared as control and blank, respectively.  
177 All the tests were prepared in triplicates, flushed with N<sub>2</sub>, sealed with rubber stoppers  
178 and aluminum caps and incubated at 55 °C and 155 rpm.

179

## 180 **3. Results And Discussion**

### 181 **3.1 Process performances and biogas upgrade**

182 Operational data from upgrading (R1) and control (R2) reactor under steady state  
183 conditions are reported in Table 1 and 2.

184

#### 185 **3.1.1 Period I: the pre H<sub>2</sub> phase**

186 In the pre H<sub>2</sub> phase (Period I), the two reactors showed similar performance in terms of  
187 biogas production rate (on average 2147 mL/L-reactor.day) and CH<sub>4</sub> yield (335  
188 mL/gVS, corresponding to ~70% of the theoretical) (Table 1). This result is in  
189 accordance with previous studies on biogas production from starch biomasses (Frigon  
190 and Guiot, 2010). The average CH<sub>4</sub> content of the reactors was ~59% (Table 1 and Fig.  
191 1), the pH was ~7.5 and the total VFA content >1 g/L (Table 1 and Fig. 2).

192

193 **3.1.2 Period II: effect of rashig rings as H<sub>2</sub> distribution device on biogas upgrading**  
194 **performance**

195 To increase the  $k_L a$  and thereby enhance gas-liquid transfer, rashig rings were placed in  
196 the H<sub>2</sub>-injection chamber to break H<sub>2</sub> bubbles and thus increase contact surface area  
197 between gas and liquid phases (Kramer and Bailey, 1991). Once steady state conditions  
198 were achieved, H<sub>2</sub> was continuously injected (3.5 L/L.day), through a metallic diffuser,  
199 in the H<sub>2</sub>-injection chamber (In-situ phase). By comparing reactors' performance, in R1,  
200 45% higher CH<sub>4</sub> production rate was observed (Table 1 and Fig. 3). Additionally, a pH  
201 increase to 7.9 was recorded in R1, as a result of the CO<sub>2</sub> removal (Table 1 and Fig. 2a).  
202 Nevertheless, because of the low H<sub>2</sub> gas-liquid mass transfer rate, only 51% of the H<sub>2</sub>  
203 injected was utilized leading to a high amount of unutilized H<sub>2</sub> in the output gas (45%)  
204 (Table 1 and Fig 1a). Additionally, a remarkable increase in VFA levels, reaching 3.4  
205 g/L, was recorded in the upgrading reactor, while VFA concentration in the control  
206 reactor remained stable (Table 1 and Fig. 2b). This is likely due to the high H<sub>2</sub> partial  
207 pressure that affected negatively acidogenic VFA conversion resulting in their  
208 accumulation. Moreover, the continuous H<sub>2</sub> injection led to a progressive higher H<sub>2</sub>  
209 partial pressure, which shifted the metabolic pathway towards homoacetogenesis  
210 inhibiting methanogenesis (Cord-Ruwisch et al., 1997). This argument was supported  
211 by the predominance and accumulation of acetate over other VFA in R1 accounting for  
212 55% of total VFA (Table 1). Moreover, this level was 4 % higher than the  
213 correspondent level in R2, which, together with higher total VFA concentrations,  
214 demonstrates the instability caused by the excessive H<sub>2</sub> flow rate provided in R1.  
215 Therefore, to provide a more accurate estimation of the increment of the CH<sub>4</sub> production  
216 rate due to CO<sub>2</sub> and H<sub>2</sub> conversion, the total VFA concentrations in the two systems

217 were converted in equivalent  $\text{CH}_4$  production, as described in section 2.2. The difference  
218 in the VFA concentration between the two reactors was taken into account to estimate  
219 the inhibition of liquid substrate degradation occurring in the upgrading reactor and  
220 allow the reactors' performances to be comparable. Thus, the  $\text{CH}_4$  derived from  $\text{CO}_2$  and  
221  $\text{H}_2$  conversion was calculated (equation 3) based on the difference between the  $\text{CH}_4$   
222 production rates of the two systems after normalization of VFA.

223 To overcome the negative effect of the  $\text{H}_2$  on the biomethanation process and improve  
224 the  $\text{H}_2$  consumption, in the last part of this period the  $\text{H}_2$  flow rate was reduced to 2.6  
225 L/L.day reducing the unutilized  $\text{H}_2$  to 34% of the output gas and increasing the  $\text{CH}_4$   
226 content to 47%.

227

### 228 **3.1.3 Period III: effect of liquid recirculation on upgrading performance**

229 Good mixing is known to be crucial to make substrates available for microorganisms  
230 (Bhattacharyya and Singh, 2010; Luo and Angelidaki, 2012). Moreover good mixing  
231 increases the  $k_L a$  for gasses, which is function of the surface area per unit volume,  
232 thereby increasing gas-liquid contact (Kramer and Bailey, 1991). Therefore, to improve  
233  $\text{H}_2$ -liquid contact, the liquid recirculation flow was increased from 4 to 7 L/h, while the  
234  $\text{H}_2$  flow rate was maintained to 2.6 L/L.day leading to a slight increase of the utilized  $\text{H}_2$   
235 (53%) (Table1). The unutilized  $\text{H}_2$  and the  $\text{CH}_4$  content in the output gas stabilized to  
236 37% and 45%, respectively (Table 1 and Fig. 1a). Similarly, in this period in R1 36%  
237 higher  $\text{CH}_4$  production rate was recorded, compared to R2 (Table 1 and Fig. 3). As these  
238 results did not markedly differ from the last part of period I (i.e.  $\text{H}_2$  flow rate was  
239 reduced to 2.6 L/L.day), it can be concluded that the improved upgrading efficiency was  
240 mainly attributed to the lower  $\text{H}_2$  flow rate applied, rather than to the higher liquid

241 recirculation flow. In fact, upon H<sub>2</sub> addition, the granular bed appeared less expanded,  
242 probably due to reduced dissolved CO<sub>2</sub> concentration in the liquid, due to the  
243 hydrogenotrophic consumption of CO<sub>2</sub> to CH<sub>4</sub> (Ohsumi et al., 1992; Song et al., 2005).  
244 Therefore, the positive effect of the higher liquid recirculation on biogas production and  
245 upgrading was not achieved.

246

#### 247 **3.1.4 Period IV: effect of alumina ceramic sponge as H<sub>2</sub> distribution device on** 248 **upgrading performance**

249 An alternative method to reduce H<sub>2</sub> bubbles size and thus increase gas-liquid contact  
250 is by increasing the surface area of the material over which the bubbles travelled and  
251 thereby breaking them to a smaller size. Based on that, the rashig rings in the H<sub>2</sub>-  
252 injection chamber were replaced with alumina ceramic sponge. Alumina ceramic  
253 sponge introduced in the chamber had 16 m<sup>2</sup> (0.3 m<sup>2</sup>/g) surface area which is  
254 significantly higher compared to the surface area in rashig rings (0.1 m<sup>2</sup>, corresponding  
255 to 0.002 m<sup>2</sup>/g). Interestingly, in this period, the H<sub>2</sub> utilization and the CH<sub>4</sub> production  
256 rate derived from CO<sub>2</sub> and H<sub>2</sub> conversion increased (Table 1 and Fig. 3). On average,  
257 67% of the H<sub>2</sub> injected was utilized reducing the H<sub>2</sub> content in the output gas to 31%  
258 and increasing the CH<sub>4</sub> content to 52% (Table 1 and Fig. 1a). These results clearly show  
259 the influence of the H<sub>2</sub> distribution on the upgrading performances indicating the  
260 importance of porosity and pore size of the H<sub>2</sub> distribution device for an effective H<sub>2</sub>  
261 utilization by microorganisms.

262 In this period lower biogas and CH<sub>4</sub> production rates were observed in particular in  
263 R2 (Table 1 and Fig. 3). Previous studies have demonstrated that aluminum oxide does  
264 not cause any toxic effects on microorganisms' growth (Ingham et al., 2012).

265 Additionally, state indicators of the biomethanation process, such as VFA and pH, did  
266 not demonstrate any imbalance. More specifically, the VFA levels recorded in this  
267 period and particularly for R1 were at the lowest levels compared to the other periods  
268 (Table 1 and Fig. 2b). Therefore, we assume that ceramic sponge pores could have  
269 retained undigested biomass particles with consequent decrease of CH<sub>4</sub> production.

270 In the last part of this period, in order to reduce the unutilized H<sub>2</sub>, the H<sub>2</sub> flow rate was  
271 further decreased to 2 L/L.day resulting in reduced H<sub>2</sub> and increased CH<sub>4</sub> content in the  
272 output gas to 20% and 57%, respectively.

273

### 274 **3.1.5 Period V and VI: effect of gas recirculation on upgrading performance**

275 As previously described, gas recirculation would have a positive effect on  $k_L a$   
276 coefficient, increasing H<sub>2</sub> gas-liquid mass transfer rate (Equation 1) (Guiot et al., 2011).

277 Therefore, in period V, 4 mL/min gas recirculation (then increased to 6 mL/min, in  
278 period VI) were applied to R1 improving the H<sub>2</sub> dissolution and thus significantly  
279 increasing the CO<sub>2</sub> conversion. In fact, in these periods on average 87% of the H<sub>2</sub>  
280 injected was utilized leading to 37% higher CH<sub>4</sub> production rate (Table 2 and Fig. 3).  
281 Nevertheless, an increase in the pH value to 8.2 was recorded as a result of the CO<sub>2</sub>  
282 removal (Table 2 and Fig. 2a). The CH<sub>4</sub> content in the biogas markedly increased to  
283 66% and the unutilized H<sub>2</sub> decreased to 14% (Table 2 and Fig. 1a). To further decrease  
284 the unutilized H<sub>2</sub>, at the end of the period the H<sub>2</sub> flow rate was reduced to 1.8 L/L.day  
285 (corresponding to ~2.5 times the CO<sub>2</sub> production rate recorded in R2). Nevertheless, no  
286 substantial difference in biogas composition and upgrading performances was recorded.  
287 In previous studies, H<sub>2</sub> distribution in the reactor's liquid phase was optimized by the  
288 application of gas recirculation flow rates ~4-folds higher than the input gas flow rate

289 (Díaz et al., 2015). Unfortunately, in this experiment, beside the positive effect on  
290 upgrading performances, the application of such a high gas recirculation flow rate led to  
291 an excessive pressure through the diffuser and to turbulent movements causing granules  
292 disintegration. The subsequent reduction of reactor's active biomass can explain the  
293 lower CH<sub>4</sub> production rate and VFA levels higher than 5 g/L observed in R1 from  
294 period V (Table 2, Fig. 2b and Fig. 3).

295

### 296 **3.1.6 Period VII and VIII: Effect of gas retention time using H<sub>2</sub>-injection chamber** 297 **configuration on upgrading process performance**

298 To increase the contact area between H<sub>2</sub> bubbles and liquid, and therefore increase H<sub>2</sub>  
299 transfer coefficient (Equation 1), the ceramic sponge surface area was doubled. This  
300 was done by doubling H<sub>2</sub>-injection chamber volume, either by connecting two chambers  
301 in series (Period VII), or by assembling them in a single longer chamber (Period VIII).  
302 The connection of two chambers in series did not lead to a substantial improvement of  
303 upgrading performances, indicating that chamber's volume itself has not a direct  
304 correlation with H<sub>2</sub> distribution. Nevertheless, by assembling two chambers in a single  
305 longer one, a higher H<sub>2</sub> percentage was utilized (94%) resulting in only 8% H<sub>2</sub>  
306 unutilized (Table 2 and Fig. 1a). Therefore, CO<sub>2</sub> and CH<sub>4</sub> contents in the output biogas  
307 dropped to 10% and increased to 81% (with a maximum of 82%) respectively (Table 2  
308 and Fig. 1a). However, in this period the pH raised to 8.4 as a consequence of the high  
309 CO<sub>2</sub> conversion (Table 2 and Fig. 2a). The results clearly demonstrate the importance of  
310 a proper reactor configuration design that increases the gas retention time leading to  
311 more efficient H<sub>2</sub> distribution and CO<sub>2</sub> conversion to CH<sub>4</sub>.

312 Moreover, from the comparison of reactors CH<sub>4</sub> production rate, it was shown that, in  
313 the upgrading reactor, on average the CH<sub>4</sub> produced from the conversion of CO<sub>2</sub>  
314 represented ~37% of the total recorded CH<sub>4</sub> production rate (Table 1 and 2 and Fig. 3).

315 Finally, it should be mentioned that the lower CH<sub>4</sub> production and higher VFA levels  
316 of control reactor observed in period VII were due to the disassembly of the separate  
317 chamber in order to be mounted in the upgrading reactor (Table 2 and Fig. 2b and 3).

318 The CH<sub>4</sub> productivity and the VFA concentration of the control reactor were recovered  
319 in period VIII.

320

### 321 **3.2 Specific methanogenic activity test**

322 H<sub>2</sub> addition is known to promote the hydrogenotrophic methanogenic pathway (Bassani  
323 et al., 2015; Luo and Angelidaki, 2013a, 2013b). Therefore, in this experiment, SMA  
324 tests were performed to validate the effect of the H<sub>2</sub> addition on methanogenesis  
325 pathways. Granules and liquid samples were taken from the reactors at steady state of  
326 periods IV (introduction of ceramic sponge as H<sub>2</sub> distribution device) and V  
327 (application of gas recirculation). It was shown that the preferable methanogenic  
328 pathway in both reactors (i.e. R1 and R2) was hydrogenotrophic (Table 3). This result  
329 was expected because hydrogenotrophic methanogens are known to be predominant in  
330 starch-grown granules (Lu et al., 2015).

331 In period IV, CH<sub>4</sub> production rate achieved by batches fed with H<sub>2</sub>/CO<sub>2</sub> did not show  
332 markedly difference between the two reactors. Conversely, in period V, higher  
333 hydrogenotrophic activity was observed in R1 compared to the control reactor, likely  
334 due to the gas recirculation enhancing the effect of H<sub>2</sub> addition on microbial community  
335 composition and thus stimulating hydrogenotrophic methanogenic pathway.



336 Both tests showed low acetoclastic activity which can be explained by the high acetate  
337 levels detected in the reactors before the tests which further increased in period V (~3.3  
338 g/L in R1 and ~1.5 g/L in R2; Table 2). Moreover, by comparing the concentration of  
339 unutilized acetate at the end of SMA tests and in the UASB reactors, it was shown that  
340 acetate levels markedly decreased in all batches (from 3 to 2.5 g/L in the upgrading  
341 system and from 1.4 to 1.3 g/L in the control treatment), apart from batches fed with  
342 acetate, where acetate levels increased to 3.3 and 1.8 g/L in R1 and R2, respectively.  
343 These results indicate that high acetate levels in the inoculum obtained from the reactor  
344 probably inhibited the process not allowing the further degradation of the supplemental  
345 amount of acetate that was added in the batch bottles (Gorris et al., 1989).  
346 Finally, it was found that the specific microbial activity for the degradation of glucose  
347 was lower in period V compared to period IV. This could be possibly due to the  
348 negative effect of gas recirculation on the granules as previously discussed in the  
349 continuous reactor operation (Tables 1, 2 and 3).

350

#### 351 **4. Conclusions**

352 The current research demonstrated the feasibility of in-situ biogas upgrading using an  
353 external chamber with 25% of the conventional biogas reactor volume. Key factors  
354 affecting the H<sub>2</sub> gas-liquid mass transfer rate were tested to improve the efficiency of  
355 the overall process. It was shown that the use of porous devices benefit the H<sub>2</sub> uptake as  
356 the active contact area is increasing and the gas retention time is extended. Moreover,  
357 the gas recirculation flow rate and the chamber design are fundamental elements that  
358 must be considered to maximize the gas retention time and thus the H<sub>2</sub> dissolution to the  
359 liquid media.

360

## 361 **Acknowledgments**

362 We thank Hector Garcia and Hector Diaz for technical assistance. This work was  
363 supported by the Danish Council for Strategic Research under the project “SYMBIO–  
364 Integration of biomass and wind power for biogas enhancement and upgrading via  
365 hydrogen assisted anaerobic digestion”, contract 12-132654.

366

## 367 **Appendix A. Supplementary data**

368 Supplementary data associated with this article can be found, in the online version, at

369

370

## 371 **References**

- 372 1. Abeling, U., Seyfried, C.F., 1993. Anaerobic-aerobic treatment of potato-starch  
373 wastewater. *Water Sci. Technol.* 28, 165–176.
- 374 2. APHA, 2005. *Standard Methods for the Examination of Water and Wastewater*,  
375 American Water Works Association/American Public Works Association/Water  
376 Environment Federation.
- 377 3. Barampouti, E.M.P., Mai, S.T., Vlyssides, A.G., 2005. Dynamic modeling of biogas  
378 production in an UASB reactor for potato processing wastewater treatment. *Chem.*  
379 *Eng. J.* 106, 53–58.
- 380 4. Bassani, I., Kougias, P.G., Treu, L., Angelidaki, I., 2015. Biogas Upgrading via  
381 Hydrogenotrophic Methanogenesis in Two-Stage Continuous Stirred Tank Reactors  
382 at Mesophilic and Thermophilic Conditions. *Environ. Sci. Technol.* 49, 12585-  
383 12593.

- 384 5. Bhattacharyya, D., Singh, K.S., 2010. Understanding the Mixing Pattern in an  
385 Anaerobic Expanded Granular Sludge Bed Reactor: Effect of Liquid Recirculation.  
386 J. Environ. Eng. 136, 576–584.
- 387 6. Cord-Ruwisch, R., Merz, T.I., Hoh, C.Y., Strong, G.E., 1997. Dissolved hydrogen  
388 concentration as an on-line control parameter for the automated operation and  
389 optimization of anaerobic digesters. Biotechnol. Bioeng. 56, 626–634.
- 390 7. Deng, L., Hägg, M.B., 2010. Techno-economic evaluation of biogas upgrading  
391 process using CO<sub>2</sub> facilitated transport membrane. Int. J. Greenh. Gas Control. 4,  
392 638–646.
- 393 8. Díaz, I., Pérez, C., Alfaro, N., Fdz-Polanco, F., 2015. A feasibility study on the  
394 bioconversion of CO<sub>2</sub> and H<sub>2</sub> to biomethane by gas sparging through polymeric  
395 membranes. Bioresour. Technol. 185, 246–53.
- 396 9. Frigon, J.C., Guiot, S.R., 2010. Biomethane production from starch and  
397 lignocellulosic crops: A comparative review. Biofuels, Bioprod. Biorefining. 4, 447-  
398 458.
- 399 10. Gomec, C.Y., 2010. High-rate anaerobic treatment of domestic wastewater at  
400 ambient operating temperatures: A review on benefits and drawbacks. J. Environ.  
401 Sci. Health. A. Tox. Hazard. Subst. Environ. Eng. 45, 1169–1184.
- 402 11. Gorris, L.G.M., van Deursen, J.M.A., van der Drift, C., Vogels, G.D., 1989.  
403 Inhibition of propionate degradation by acetate in methanogenic fluidized bed  
404 reactors. Biotechnol. Lett. 11, 61–66.
- 405 12. Guiot, S.R., Cimpoia, R., Carayon, G., 2011. Potential of wastewater-treating  
406 anaerobic granules for biomethanation of synthesis gas. Environ. Sci. Technol. 45,  
407 2006–2012.

- 408 13. Ingham, C.J., ter Maat, J., de Vos, W.M., 2012. Where bio meets nano: The many  
409 uses for nanoporous aluminum oxide in biotechnology. *Biotechnol. Adv.* 30, 1089-  
410 1099.
- 411 14. Kougias, P.G., Boe, K., Einarsdottir, E.S., Angelidaki, I., 2015. Counteracting  
412 foaming caused by lipids or proteins in biogas reactors using rapeseed oil or oleic  
413 acid as antifoaming agents. *Water Res.* 79, 119–27.
- 414 15. Kramer, H.W., Bailey, J.E., 1991. Mass transfer characterization of an airlift probe  
415 for oxygenating and mixing cell suspensions in an NMR spectrometer. *Biotechnol.*  
416 *Bioeng.* 37, 205–209.
- 417 16. Lu, X., Zhen, G., Estrada, A.L., Chen, M., Ni, J., Hojo, T., Kubota, K., Li, Y.Y.,  
418 2015. Operation performance and granule characterization of upflow anaerobic  
419 sludge blanket (UASB) reactor treating wastewater with starch as the sole carbon  
420 source. *Bioresour. Technol.* 180, 264–273.
- 421 17. Luo, G., Angelidaki, I., 2012. Integrated biogas upgrading and hydrogen utilization  
422 in an anaerobic reactor containing enriched hydrogenotrophic methanogenic culture.  
423 *Biotechnol. Bioeng.* 109, 2729–2736.
- 424 18. Luo, G., Angelidaki, I., 2013. Co-digestion of manure and whey for in situ biogas  
425 upgrading by the addition of H<sub>2</sub>: Process performance and microbial insights. *Appl.*  
426 *Microbiol. Biotechnol.* 97, 1373–1381.
- 427 19. Luo, G., Johansson, S., Boe, K., Xie, L., Zhou, Q., Angelidaki, I., 2012.  
428 Simultaneous hydrogen utilization and in situ biogas upgrading in an anaerobic  
429 reactor. *Biotechnol. Bioeng.* 109, 1088–1094.

- 430 20. Muñoz, R., Meier, L., Diaz, I., Jeison, D., 2015. A review on the state-of-the-art of  
431 physical/chemical and biological technologies for biogas upgrading. *Rev. Environ.*  
432 *Sci. Biotechnol.* 14, 727-759.
- 433 21. Nizami, A.S., Orozco, A., Groom, E., Dieterich, B., Murphy, J.D., 2012. How much  
434 gas can we get from grass? *Appl. Energy.* 92, 783–790.
- 435 22. Nordberg, Å., Edström, M., Uusi-Penttilä, M., Rasmuson, Å.C., 2012. Selective  
436 desorption of carbon dioxide from sewage sludge for in-situ methane enrichment:  
437 Enrichment experiments in pilot scale. *Biomass and Bioenergy.* 37, 196–204.
- 438 23. Ohsumi, T., Nakashiki, N., Shitashima, K., HIRAMA, K., 1992. Density change of  
439 water due to dissolution of carbon dioxide and near-field behavior of CO<sub>2</sub> from a  
440 source on deep-sea floor. *Energy Convers. Manag.* 33, 685–690.
- 441 24. Pauss, A., Andre, G., Perrier, M., Guiot, S.R., 1990. Liquid-to-Gas mass transfer in  
442 anaerobic processes: Inevitable transfer limitations of methane and hydrogen in the  
443 biomethanation process. *Appl. Environ. Microbiol.* 56, 1636–1644.
- 444 25. Powar, M.M., Kore, V.S., Kore, S. V, Kulkarni, G.S., 2013. Review on Applications  
445 of Uasb Technology for Wastewater Treatment. *Int. J. Adv. Sci. Eng. Technol.* 2,  
446 125–133.
- 447 26. Sevilla-Espinosa, S., Solórzano-Campo, M., Bello-Mendoza, R., 2010. Performance  
448 of staged and non-staged up-flow anaerobic sludge bed (USSB and UASB) reactors  
449 treating low strength complex wastewater. *Biodegradation.* 21, 737–751.
- 450 27. Song, Y., Chen, B., Nishio, M., Akai, M., 2005. The study on density change of  
451 carbon dioxide seawater solution at high pressure and low temperature. *Energy.* 30,  
452 2298–2307.

- 453 28. Weiland, P., 2010. Biogas production: current state and perspectives. Appl.  
454 Microbiol. Biotechnol. 85, 849–860.
- 455 29. Zheng, M.X., Wang, K.J., Zuo, J.E., Yan, Z., Fang, H., Yu, J.W., 2012. Flow pattern  
456 analysis of a full-scale expanded granular sludge bed-type reactor under different  
457 organic loading rates. Bioresour. Technol. 107, 33–40.

458 **Table captions:**

459 **Table 1:** Upgrading (R1) and control (R2) reactor performances under steady state  
460 conditions (Periods I-IV).

461 **Table 2:** Upgrading (R1) and control (R2) reactor performances under steady state  
462 conditions (Periods V-VIII).

463 **Table 3:** Specific methanogenic activity (SMA) results, expressed as CH<sub>4</sub> production  
464 rate (mL/L.day), under steady state conditions.

465 **Figure captions:**

466 **Fig. 1:** Biogas composition ( $\text{CH}_4$  (●),  $\text{CO}_2$  (○) and  $\text{H}_2$  (■) %) of (a) upgrading and (b)  
467 control reactor.

468 **Fig. 2:** pH (a) and total VFA (b) of upgrading (◆) and control (○) reactor.

469 **Fig. 3:**  $\text{CH}_4$  production rate of upgrading (◆) and control (○) reactor.



**Table 1**

Phase	Pre H <sub>2</sub>				In-situ			
	I		II		III		IV	
H <sub>2</sub> distribution device	-		rashig rings		rashig rings		ceramic sponge	
Reactor	R1	R2	R1	R2	R1	R2	R1	R2
Liquid recirculation flow (L/h)	4	4	4	4	7	7	7	7
Gas recirculation flow (mL/min)	NA*	/	NA*	/	NA*	/	NA*	/
Biogas production rate (mL/L.day)	2167±180	2127±180	2093±232	2229±129	2072±102	2015±75	1953±97	1787±57
Biogas composition (%):								
CH <sub>4</sub>	58.2±3.4	60.3±3.0	40.4±4.3	60.6±1.8	44.9±2.3	60.9±1.0	52.0±1.9	62.5±0.3
CO <sub>2</sub>	41.8±3.4	39.7±3.0	14.9±3.2	39.4±1.8	18.5±3.2	39.1±1.0	17.0±0.7	37.5±0.3
H <sub>2</sub>	NA*	/	44.6±6.7	/	36.6±1.9	/	31.0±1.9	/
CH <sub>4</sub> production rate (mL/L.day)	1255±54	1277±61	1528±147	1350±74	1497±73	1227±53	1471±72	1117±39
CO <sub>2</sub> in output gas (mL/L.day)	912±148	850±134	565±115	878±73	618±55	789±33	482±34	670±19

H <sub>2</sub> flow rate (mL/L.day)	NA*	/	3477±594	/	2636±89	/	2629±93	/
H <sub>2</sub> consumption rate (mL/L.day)	NA*	/	1769±330	/	1412±212	/	1756±121	/
pH	7.46±0.03	7.49±0.06	7.92±0.11	7.59±0.09	7.90±0.06	7.60±0.05	7.93±0.12	7.56±0.09
Total VFA (g/L)	1.69±0.37	1.21±0.25	3.40±0.31	1.41±0.28	3.60±0.23	2.26±0.11	2.81±0.46	2.37±0.32
Acetate content in VFA (%)	41.3±4.3	49.0±3.9	55.3±4.0	51.5±3.8	51.8±2.3	47.3±3.7	49.7±3.8	47.2±4.2

---

\*NA: not applicable to this period

**Table 2**

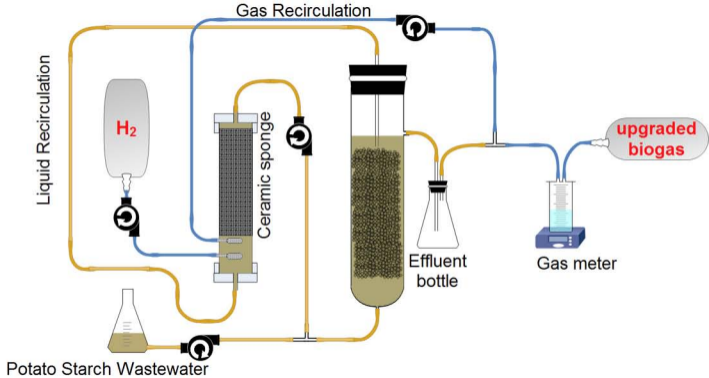
Phase	In-situ							
Period	V		VI		VII		VIII	
H <sub>2</sub> distribution device	ceramic sponge		ceramic sponge		serial chambers		single chamber with extended length	
Reactor	R1	R2	R1	R2	R1	R2	R1	R2
Liquid recirculation flow (L/h)	7	7	7	7	7	7	7	7
Gas recirculation flow (mL/min)	4	/	6	/	6	/	6	/
Biogas production rate (mL/L.day)	1786±68	1900±85	1521±98	2018±275	1337±72	1175±138	1261±157	1558±188
Biogas composition (%):								
CH <sub>4</sub>	66.4±1.9	61.1±1.2	66.0±2.5	65.0±2.4	67.6±2.0	65.0±1.0	81.3±0.6	66.7±2.8
CO <sub>2</sub>	20.5±4.0	38.9±1.2	18.35±3.9	35.0±2,4	18.8±0.5	35.0±1.0	10.2±1.0	33.2±2.8
H <sub>2</sub>	13.0±4.3	/	15.7±1.4	/	13.5±2.4	/	8.5±1.5	/
CH <sub>4</sub> production rate (mL/L.day)	1365±52	1161±55	1188±55	1308±149	1046±57	763±92	1145±134	1039±121

CO <sub>2</sub> in output gas (mL/L.day)	421±65	740±47	333±82	710±134	291±16	412±48	121±21	615±83
H <sub>2</sub> flow rate (mL/L.day)	2144±312	/	1834±30	/	1768±55	/	1828±14	/
H <sub>2</sub> consumption rate (mL/L.day)	1873±234	/	1551±44	/	1536±80	/	1717±23	/
pH	7.83±0.10	7.64±0.07	8.24±0.20	7.85±0.12	8.18±0.08	7.92±0.07	8.38±0.07	7.99±0.09
Total VFA (g/L)	5.11±0.06	3.24±0.48	3.66±0.97	2.37±0.27	4.34±0.40	3.21±0.39	3.87±0.40	2.36±0.15
Acetate content in VFA (%)	64.6±3.4	46.0±4.7	39.9±2.6	39.4±4.3	37.0±2.2	36.5±2.9	30.3±1.4	34.5±6.5

---

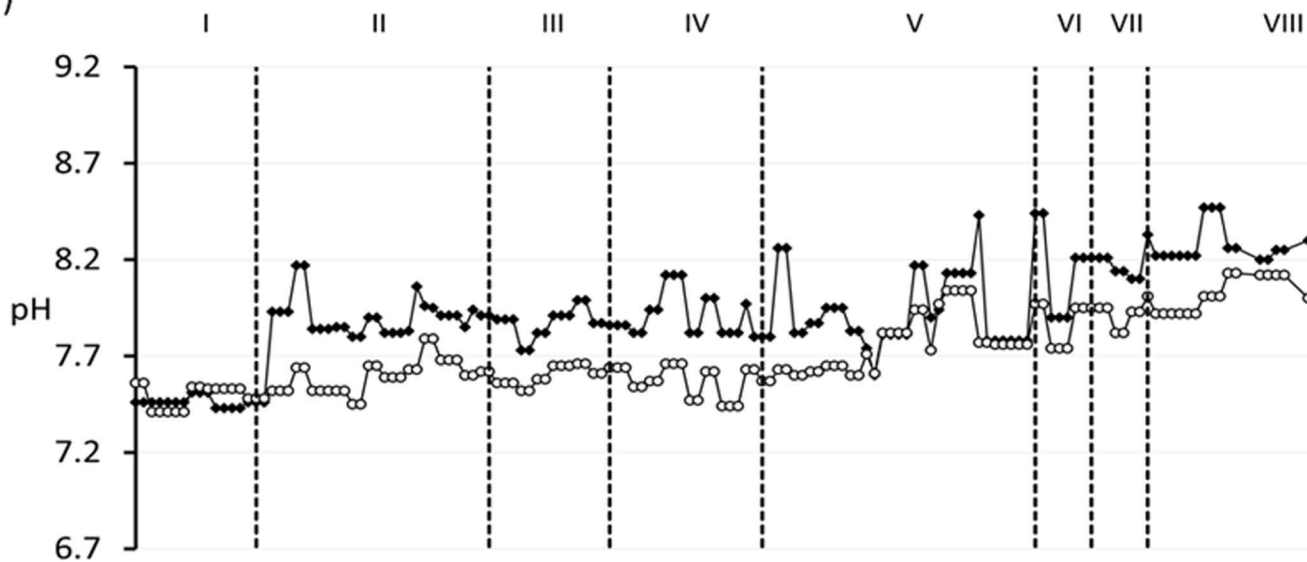
**Table 3**

Period	IV		V	
Reactor	R1	R2	R1	R2
Blank	36±2	11±2	6±1	7±1
Glucose	589±67	219±6	73±22	23±12
Acetate	159±4	4±1	4±1	3±2
H <sub>2</sub> /CO <sub>2</sub>	1270±20	1296±29	986±212	520±65





a)



b)

